Improved photovoltaic performance of 2D-conjugated benzodithiophene-based polymer by the side chain engineering at quinoxaline

Qunping Fan [a], Manjun Xiao [a], Yu Liu [a,*], Wenyan Su [a], Huishan Gao [a], Hua Tan [a],

Yafei Wang [a], Gangtie Lei [a], Renqiang Yang [b,*], Weiguo Zhu [a,*]

[a] *College of Chemistry, Xiangtan University, Key Lab of Environment-Friendly*

Chemistry and Application in Ministry of Education, Xiangtan 411105, China

[b] *Qingdao Institute of Bioenergy and Bioprocess Technology, Chinese Academy of*

Sciences, Qingdao 266101, China

Corresponding author: Prof. Yu Liu; Renqiang Yang; Weiguo Zhu

Tel: +86-731-58293377

Fax: +86-731-58292251

E-mail addresses: liuyu03b@126.com; yangrq@qibebt.ac.cn; zhuwg18@126.com

Abstract: To investigate the influence of side chains at quinoxaline on the photovoltaic performances, a novel D-A-type polymer of PBDTDT(Qx-3)-T was synthesized and characterized, in which 5,8-dioctylthienyl substituted benzo[1,2-*b*:4,5-*b'*]dithiophene (BDT-T), thiophene (T) and 6,7-dioctyloxy-2,3-diphenylquinoxaline (Qx-3) were used as the donor (D) unit, π-bridge and acceptor (A) unit, respectively. The resultant polymer exhibited good thermal stability with a high decomposition temperature of 357 ^{o}C, a low optical bandgap of 1.78 eV with an absorption onset of 696 nm, a low-lying highest occupied molecular orbital (HOMO) energy level of -5.51 eV, and a high carrier mobility of 2.19×10^{-4} cm^{2} V^{-1} s^{-1}. Compared to the reported analogues, polymer solar cells (PSCs) based on PBDTDT(Qx-3)-T/PC$_{71}$BM demonstrated the highest open-circuit voltages (V_{oc}) up to 0.96 V. The maximum power conversion efficiency (PCE) of 6.9% with a V_{oc} of 0.94 V, short-circuit current (J_{sc}) of 11.28 mA cm^{-2} and fill factor (*FF*) of 64.7% was obtained with a delicate balance among the above factors for the polymer in PSCs. On the basis of these results, it can be concluded that the appending two octyloxy side chains at 6,7-positions of quinoxaline in the BDT-T-*alt*-DTQx type polymers would be a feasible approach to improve photovoltaic properties.

KEYWORDS: Benzo[1,2-*b*:4,5-*b'*]dithiophene; Quinoxaline; Polymer solar cells; Donor-acceptor; Side chains

1. Introduction

As a promising sustainable energy source technology for future, polymer solar cells (PSCs) have recently attracted tremendous interest due to their advantages of low cast, light weight, flexibility, and ease of processing, which leads to the realization of next-generation renewable energy sources.[1-4] To improve photovoltaic performance of PSCs, numerous attempts have been devoted to develop new solution processable donor-acceptor (D-A)-type polymer donor materials with narrow optical bandgap [5-9] More encouragingly, PSCs with high-record power conversion efficiencies (PCEs) up to 10.8% were reported.[10] Despite some remarkable advancements of the polymer donor materials were achieved, high efficient PSCs remains some challenges, especially with respect to high-lying the highest occupied molecular orbital (HOMO) levels lead to low open-circuit voltages (V_{oc}), narrow absorption spectra lead to small short-circuit current (J_{sc}), and low carrier mobility lead to weak fill factor (FF).[11-13] Based on the previous reports,[11,14-16] the PCEs of the PSCs are proportional to three parameters interplay each other (V_{oc}, J_{sc} and FF). For example, V_{oc} is mainly related to the energy level between the HOMO of the polymer donor materials and the lowest unoccupied molecular orbital (LUMO) of the fullerene acceptor materials.[11] However, a lower HOMO level of the polymer donor materials would reduce FF, increase optical bandgap and decrease J_{sc}.[11,17] That is, high V_{oc}, J_{sc} and FF are difficult to obtain concurrently.[18] Obviously, a delicate balance among these three factors of the optical bandgap, energy level and carrier mobility is needed via sophisticated control over the physical properties of a donor material to achieve higher PCEs in PSC.

Recently, 7,8-dithienyl substituted benzo[1,2-*b*:4,5-*b′*]dithiophene (BDT-T) have been flourishing as electron donor units for application in PSCs, due to its relatively large and planar conjugated structure that are favorable for π-π stacking, improvement of carrier transportation and absorption in long wavelengths.[19-25] So far in the literature, a record PCE of 10.2% was obtained in the BDT-T polymer based device by Hou group.[19] Meanwhile, another effective way to promote physical properties of conjugated polymer is to introduce conjugating components of quinoxaline derivatives with strong quinoid property, due to their relatively stable and strong electron withdrawing properties that are conducive to promoting the intramolecular charge transfer (ICT) effect, which endow them with a broader light absorption and enhanced carrier transportation.[26-29] A notable PCE up to 8.0% with J_{sc} of 18.2 mA cm^{-2} was obtained in the quinoxaline-polymer based device by Chou group.[29] Further, to explore the interactions between the BDT-T and 5,8-dithienylquinoxaline (DTQx) in polymers, there are some exciting reports about the BDT-T-*alt*-DTQx-based polymers recently.[30-34] For instance, Hou *et al.* reported a polymer of PBDTDTQx-T with an alternating D-A backbone of BDT-T-*alt*-2,3-di(3-alkyloxyphenyl)-DTQx.[32] To further study the effect of various substituted side chains on photovoltaic properties of these BDT-T-*alt*-DTQx polymers, our group recently reported two other polymers of PBDTT-TQ with an alternating D-A backbone of BDT-T-*alt*-6,7-difluoro-2,3-di(3-alkyloxyphenyl)-DTQx and PBDTDT(Qx-2)-T with an alternating D-A backbone of BDTT-*alt*-6,7-dialkyloxy-2,3-di(4-alkyloxyphenyl)-DTQx,[33,34] respectively. Recently, some significant influences of various substituted side chains at 6,7-positions of

quinoxaline on PCE of these polymers based devices were also observed, while the

phenyl has two alkoxy groups. For example, PBDTDTQx-T with two hydrogen

atoms at 6,7-positions of quinoxaline was found to show a relatively low V_{oc} of 0.76 V,

low J_{sc} of 10.13 mA cm^{-2} and high FF of 64.3% resulted in a poor PCE of 5.0%.[32]

PBDTT-TQ with two fluorine atoms at 6,7-positions of quinoxaline was found to

display a similarly low V_{oc} of 0.77 V, low FF of 56.0 % and high J_{sc} of 13.70 mA cm^{-2}

resulted in a moderate PCE of 5.9%.[33] PBDTDT(Qx-2)-T with two alkoxy groups at

6,7-positions of quinoxaline was found to indicate a relatively moderate J_{sc} of 10.82

mA cm^{-2}, moderate FF of 61.4 % and high V_{oc} up to 0.95 V, which resulted in a

maximum PCE of 6.3%.[34] Obviously, these previous works using conjugated

two-dimensional (2-D) side chains on the BDT-T unit as donor and various substituted

side chains at 6,7-positions of quinoxaline as acceptor not only can increase the

rigidity of the repeating unit, but also improve the performances of PSCs. However, a

delicate balance among all these three factors of J_{sc}, V_{oc} and FF has still not been

achieved in the BDT-T-*alt*-DTQx type polymers based PSCs.

In this work, a novel D-A-type polymer of PBDTDT(Qx-3)-T was synthesized and

characterized. As shown in Chart 1, compared to the reported analogic polymers,[32-34]

this polymer was just appended with two octyloxy side chains at 6,7-positions of

quinoxaline. As the literature reported, two 6,7-dioctyloxy side chains at quinoxaline

twist the polymer main chain somehow, which can reduce HOMO energy level and

improve the V_{oc}.[34-36] Meanwhile, remove the two alkoxy side chains at phenyl not

only promote the electron withdrawing ability of quinoxaline but also reduce

intermolecular steric hindrance, which can broaden the absorption spectrum to enhance the J_{sc} value and improve carrier mobility to increase the *FF* value of the polymer.[37,38] We expected that unsubstituted phenyl and two octyloxy side chains instead of two hydrogen or two fluorine atoms at 6,7-positions of quinoxaline are able to improve photovoltaic property along with a delicate balance among these three factors of J_{sc}, V_{oc} and *FF* for their polymers in PSCs due to the above corporate effect.

The synthetic routes of PBDTDT(Qx-3)-T are shown in Scheme 1. As expected, PBDTDT(Qx-3)-T shows a low HOMO energy level of -5.51 eV, narrow optical bandgap of 1.78 eV and high hole mobility of 2.19×10^{-4} cm^2 V^{-1} s^{-1}, respectively. Polymer solar cells (PSCs) based on the polymer/PC$_{71}$BM blend presented the highest V_{oc} up to 0.96 V. The highest PCE of 6.9% with a V_{oc} of 0.94 V, J_{sc} of 11.28 mA cm^{-2} and *FF* of 64.7% was achieved. Obviously, the device shows a delicate balance among the above factors, under the illumination of AM 1.5G, 100 mW cm^{-2}. To our best knowledge, the maximum PCE and *FF* values here are highest than those for the previous BDT-T-*alt*-DTQx polymeric derivatives in BHJ-PSCs. This work demonstrates that photovoltaic properties of the BDT-T-*alt*-DTQx type polymers based PSCs can significantly improve just by grafting two octyloxy side chains at 6,7-positions of quinoxaline.

2. Experimental section

2.1. Materials

Monomer 4,7-dibromo-5,6-bis(octyloxy)benzo[*c*][1,2,5]thiadiazole (**1**) and 2,5-bis(trimethytin)-7,8-bis(5-(2-ethylhexyl)thiophen-2-yl)benzo[1,2-*b*:4,5-*b′*]dithiophene

((BDT-T)Sn$_2$Me$_6$) were purchased directly from the Suna Tech Inc. The other reagents and chemicals were purchased from commercial sources (Acros, TCI) and used without further purification. Compound **2**, **3**, **DT(Qx-3)** and **DT(Qx-3)Br$_2$** were synthesized according to the reported literature.[6,34] The detailed syntheses of monomers and polymer were presented following the procedures described herein.

2.2. Characterization

Nuclear magnetic resonance (NMR) spectra were recorded on a Bruker AV-400 spectrometer using tetramethylsilane (TMS) as a reference in deuterated chloroform solution at 298 K. Mass spectrometric measurements were performed on Bruker Bifiex III MALDI-TOF. The molecular weights were determined using a Waters GPC 2410 in tetrahydrofuran (THF) via a calibration curve of polystyrene as standard. Thermogravimetric analyses (TGA) were conducted under a dry nitrogen gas flow at a heating rate of 20 $^{\circ}$C min^{-1} on a Perkin-Elmer TGA 7. UV-Vis absorption spectra were recorded on a HP-8453 UV visible system. Cyclic voltammograms (CV) were carried out on a CHI660A electrochemical work station with a three electrode electrochemical cell in a 0.1 M tetrabutylammonium hexafluorophosphate (TBAPF$_6$) acetonitrile solution with a scan 100 mV s^{-1} at room temperature (RT) under argon atmosphere. In this three-electrode cell, a platinum rod, platinum wire and Ag/AgCl electrode were used as a working electrode, counter electrode and reference electrode, respectively. The surface morphology of the PBDTDT(Qx-3)-T/PC$_{71}$BM blend film was investigated by an atomic force microscopy (AFM) on a Veeco, DI multimode NS-3D apparatus in a tapping mode under normal air condition at RT with a 5 μm

scanner.

2.3. Fabrication and characterization of polymer solar cells

The PSCs were fabricated using indium tin oxide (ITO) glass as an anode, Ca/Al as a cathode, and a blend film of the polymer/PCBM as a photosensitive layer. After a 30 nm buffer layer of poly-(3,4-ethylenedioxy-thiophene) and polystyrene sulfonic acid (PEDOT:PSS) was spin-coated onto the precleaned ITO substrate, the photosensitive layer was subsequently prepared by spin-coating a solution of the PBDTDT(Qx-3)-T/PC$_{71}$BM (1:4, *w/w*) in 1,2-dichlorobenzene (ODCB) on the PEDOT:PSS layer with a typical concentration of 35 mg mL^{-1}, followed by annealing at 80 $^{\circ}$C for 10 minutes to remove ODCB. Ca (10 nm) and Al (100 nm) were successively deposited on the photosensitive layer in vacuum and used as top electrodes. The current-voltage (*I–V*) characterization of the devices was carried out on a computer-controlled Keithley source measurement system. A solar simulator was used as the light source and the light intensity was monitored by a standard Si solar cell. The active area was 1×10^{-2} cm^2 for each cell. The thicknesses of the spun-cast films were recorded by a profilometer (Alpha-Step 200, Tencor Instruments). The external quantum efficiency (*EQE*) was measured with a Stanford Research Systems model SR830 DSP lock-in amplifier coupled with WDG3 monochromator and a 150 W xenon lamp.

2.4. Synthesis of the monomers and polymer

2.4.1. 5,8-Dibromo-6,7-bis(octyloxy)-2,3-diphenylquinoxaline (**3**)

Compound **1** (0.55 g, 1.00 mmol) and sodium borohydride (NaBH$_4$, 0.57 g, 13.00 mmol) were mixed with ethanol (30 mL) and THF (15 mL) at 0 $^{\circ}$C, and stirred for 12

h at RT under nitrogen atmosphere. After quenched with distilled water (50 mL), the

mixture was extracted with anhydrous diethyl ether (20 mL × 3). The combined

organic layer was dried over anhydrous magnesium sulfate ($MgSO_4$) and filtered. The

filtration was distilled to remove off the solvent and the compound **2** of 2,3-diamino-

5,6-bis(octyloxy)-1,4-dibromobenzene was obtained and directly used in the next step.

To a solution of compound **2** in ethanol (20 mL) and acetic acid (40 mL) was added

benzil (0.27 g, 1.00 mmol). The mixture was refluxed under stirring for 12 h in

nitrogen atmosphere. After cooled to RT and quenched with water, the mixture was

extracted with dichloromethane (DCM, 30 mL × 3). The combined organic layer was

dried over anhydrous $MgSO_4$ and distilled to remove off solvent. The residue was

purified by silica gel column chromatography using mixed solvent of petroleum ether

(PE)-DCM (*V/V*, 2/1) as eluent to obtain compound **3** as a yellow solid (0.50 g,

72.1%). ^{1}H NMR (400 MHz, CDCl$_3$, TMS), δ (ppm): 7.64-7.62 (d, *J* = 7.1 Hz, 4H),

7.39-7.33 (m, 6H), 4.21 (t, *J* = 6.6 Hz, 4H), 1.94-1.89 (m, 4H), 1.37-1.31 (m, 20H),

0.90 (t, *J* = 5.3 Hz, 6H). MALDI-TOF MS (m/z) for $C_{36}H_{44}Br_2N_2O_2$, Calcd: 698.17,

Found: 698.19.

2.4.2. 6,7-Bis(octyloxy)-2,3-diphenyl-5,8-di(thiophen-2-yl)quinoxaline (**DT(Qx-3)**)

To a mixture of compound **3** (0.40 g, 0.57 mmol) and 2-thienyltributyltin (0.85 g,

2.28 mmol) in degassed toluene (30 mL) was added tetrakis(triphenylphosphine)-

palladium (Pd(PPh$_3$)$_4$, 0.08 g, 0.07 mmol) and then refluxed for 24 h under nitrogen

atmosphere. After cooled to RT and quenched with water, the mixture was extracted

with DCM (20 mL × 3). The combined organic layer was dried over anhydrous

$MgSO_4$ and distilled to remove off solvent. The residue was purified by silica gel column chromatography using PE-DCM (*V/V*, 2/1) as eluent to obtain **DT(Qx-3)** as a yellow solid (0.35 g, 87.3%). ^{1}H NMR (400 MHz, $CDCl_3$, TMS), δ (ppm): 8.05 (d, *J* = 3.4 Hz, 2H), 7.66-7.65 (m, 4H), 7.55 (d, *J* = 5.0 Hz, 2H), 7.33-7.32 (m, 6H), 7.21 (t, *J* = 8.0 Hz, 2H), 4.04 (t, *J* = 6.7 Hz, 4H), 1.81-1.76 (m, 4H), 1.40-1.26 (m, 20H), 0.93-0.88 (m, 6H). ^{13}C NMR (100 MHz, $CDCl_3$, TMS), (ppm): 152.87, 150.25, 138.91, 136.41, 133.47, 130.91, 130.33, 128.69, 128.17, 127.89, 126.09, 124.18, 74.10, 31.89, 30.43, 29.52, 29.34, 26.09, 22.71, 14.20. MALDI-TOF MS (m/z) for $C_{44}H_{50}N_2O_4S_2$, Calcd: 704.34, Found: 704.45.

2.4.3.   5,8-Bis(5-bromothiophen-2-yl)-6,7-bis(octyloxy)-2,3-diphenylquinoxaline

(**DT(Qx-3)Br$_2$**)

To a solution of compound **DT(Qx-3)** (0.30 g, 0.43 mmol) in THF (30 mL) was added *N*-bromosuccininide (NBS, 0.17 g, 0.95 mmol) in a two-neck round flask. The mixture was then stirred for 4 h at RT. After the solvent was distilled off, the residue was purified by silica gel column chromatography using PE-DCM (*V/V*, 2/1) as eluent to yield **DT(Qx-3)Br$_2$** as an orange solid (0.33 g, 90.1%). ^{1}H NMR (400 MHz, $CDCl_3$, TMS), δ (ppm): 7.97 (d, *J* = 3.9 Hz, 2H), 7.64 (d, *J* = 6.9 Hz, 4H), 7.37-7.36 (m, 6H), 7.15 (d, *J* = 3.8 Hz, 2H), 4.08 (t, *J* = 6.7 Hz, 4H), 1.85-1.81 (m, 4H), 1.43-1.26 (m, 20H), 0.90-0.89 (m, 6H). ^{13}C NMR (100 MHz, $CDCl_3$, TMS), (ppm): 152.68, 150.58, 138.46, 135.89, 135.19, 131.26, 130.34, 128.97, 128.91, 128.27, 123.35, 116.12, 74.23, 31.87, 30.44, 29.50, 29.33, 26.08, 22.72, 14.16. MALDI-TOF MS (m/z) for $C_{44}H_{48}Br_2N_2O_2S_2$, Calcd: 862.15, Found: 862.30.

2.4.4. Synthesis of **PBDTDT(Qx-3)-T**

In a dry 25 mL flask, tris(dibenzylideneacetone)dipalladium (Pd$_2$(dba)$_3$, 5.0 mg) and tri(*o*-tolyl)phosphine (P(*o*-Tol)$_3$, 10.0 mg) were added to a solution of **DT(Qx-3)Br$_2$** (112 mg, 0.13 mmol) and **(BDT-T)Sn$_2$Me$_6$** (100 mg, 0.13 mmol) in 6 mL degassed toluene under nitrogen and stirred vigorously at 100 $^\circ$C for 16 h. After cooled to RT, the mixture was poured into acetone (100 mL) and the precipitation was occurred. It was collected by filtration and successively extracted in Soxhlet apparatus with diethyl ether and chloroform (CHCl$_3$), respectively. The collected CHCl$_3$ solution was concentrated and precipitated with acetone to get the dark solid (135 mg, 81.3%). ^{1}H NMR (400 MHz, CDCl$_3$, TMS), δ (ppm): 8.28-8.19 (br, 2H), 7.81-7.77 (br, 6H), 7.40-8.7.34 (br, 10H), 7.00-6.98 (br, 2H), 4.14-4.13 (br, 4H), 2.95-2.94 (br, 4H), 1.87-1.76 (br, 4H), 1.75-1.73 (br, 2H), 1.48-1.27 (br, 34H), 0.99-0.86 (br, 20H). Anal. Calcd for C$_{78}$H$_{90}$N$_2$O$_2$S$_6$: C, 73.19; H, 7.09; N, 2.19; S, 15.03. Found: C, 71.32; H, 7.37; N, 2.05; S, 14.71.

3. Results and discussion

3.1. Synthesis and thermal property

As shown in Scheme 1, compound **2** was prepared through a ring-opening reaction and used immediately to obtain compound **3** via the condensation reaction with a yield of 72.1%. Compound **3** was then reacted with 2-thienyltributyltin via the Stille coupling reaction to afford **DT(Qx-3)** in the present of Pd(PPh$_3$)$_4$ with a moderate yield of 87.3%. **DT(Qx-3)** was brominated with NBS in THF to afford the monomer **DT(Qx-3)Br$_2$** with a high yield of 90.1%. The polymer of PBDTDT(Qx-3)-T was

synthesized by palladium-catalyzed Stille polymerization between **DT(Qx-3)Br$_2$** and

(BDT-T)Sn$_2$Me$_6$ with a yield of 81.3%. The chemical structures of compounds **3**,

DT(Qx-3) and **DT(Qx-3)Br$_2$** were confirmed by ^{1}H NMR, ^{13}C NMR and

MALDI-TOF mass spectroscopy (see Supporting Information). The molecular weight

of polymer was determined with GPC relative to polystyrene standards. The number

average molecular weight (M_n) of 59 kDa with a polydispersity index (PDI) of 1.64

was observed for PBDTDT(Qx-3)-T, and the related data are listed in Table 1. Due to

the influence of the appending two octyloxy side chains at quinoxaline,

PBDTDT(Qx-3)-T exhibits excellent solubility in common organic solvents, such as

CHCl$_3$, THF, chlorobenzene (CB) and ODCB.

Thermal propertiy of PBDTDT(Qx-3)-T was investigated with thermogravimetric

analysis (TGA). As shown in Fig. 1, PBDTDT(Qx-3)-T shows excellent thermal

stability, with 5% weight-loss temperatures (T_d) at 357 $^\circ$C under an inert atmosphere,

and its corresponding data is summarized in Table 1.

3.2. Optical properties

The normalized UV-Vis absorption spectra of PBDTDT(Qx-3)-T in dilute CHCl$_3$

solution with a concentration of 1×10^{-5} M and thin film are shown in Fig. 2, and the

detailed parameters are summarized in Table 2. Two typical absorption bands are

observed in the range of 340-700 nm for the polymer. The high-lying absorption band

from 340 to 450 nm is assigned to the π-π^* transition, and another low-lying

absorption band from 500 to 700 nm should be attributed to the strong ICT interaction

between the donor and acceptor units.[9] The absorption of the polymer in thin film has

about 51 nm red-shifted comparison with the absorption spectra in solution, indicating

that the stronge aggrecation is formed in the thin film. The absorption edge (λ_{onset}) of

PBDTDT(Qx-3)-T is located at 696 nm in its thin film, corresponding to the optical

band gap (E_g^{opt}) of 1.78 eV. Compared to the previous PBDTDTQx-T and PBDTT-TQ

(1.67 and 1.77 eV),[32,33] appending two octyloxy side chains to replace hydrogen or

fluorine atoms at 6,7-positions of quinoxaline, which can weaken the ICT effect to

lead a higher E_g^{opt} value and higher V_{oc} value in PSCs. A similar phenomenon has also

been reported in other literatures.[34,36] Furthermore, compared to the previous

PBDTDT(Qx-2)-T (1.82 eV),[34] two methoxy side chains were eliminated at

4,4′-positions of phenyl in PBDTDT(Qx-3)-T, which can enhance the ICT effect to

obtain a lower E_g^{opt} value and higher J_{sc} value. [37,38]

3.3. Electrochemical properties

Cyclic voltammetry (CV) was employed to investigate the electrochemical

properties of PBDTDT(Qx-3)-T by using Ag/AgCl electrode as a reference and redox

potential of ferrocene/ferrocenium (Fc/Fc$^+$) as calibrated standard. Fig. 3 shows the

recorded CV curve of PBDTDT(Qx-3)-T, and the relevant CV data are listed in Table

2. The observed onset oxidation and reduction potentials (E_{ox}/E_{red}) for

PBDTDT(Qx-3)-T are 1.16 V/-0.78 V, respectively. The HOMO and LUMO energy

levels of PBDTDT(Qx-3)-T can be calculated according to the empirical equations:[6]

$E_{HOMO} = -(E_{ox} - 0.45) - 4.8$ eV, $E_{LUMO} = -(E_{red} - 0.45) - 4.8$ eV and $E_g^{ec} = -(E_{ox} - E_{red})$ eV.

As a result, the HOMO and LUMO energy levels (E_{HOMO}/E_{LUMO}) are estimated to be

-5.51/-3.57 eV for PBDTDT-(Qx-3)-T, respectively. Obviously, PBDTDT(Qx-3)-T

presents a lower E_{HOMO} value than that of the previous analogues with two alkyloxy groups at phenyl and two fluorine (or hydrogen or octyloxy) at 6,7-positions of quinoxaline,[32-34] Obviously, increasing two octyloxy side chains at 6,7-positions of quinoxaline can twist the polymer main chain somehow and decreasing two methyloxy side chains at phenyl can enhance the electron withdrawing ability of quinoxaline caused a lower HOMO level.[34,37] The relatively deeper HOMO energy levels (5.51 eV) could be expected to afford higher V_{oc} in PSC applications, which is one of main contributors to achieve high efficiency PSCs. This discrepancy between the electrochemical and optical bandgaps might be induced by the presence of an energy barrier at the interface between the polymer neat film and the electrode surface.[39]

3.4. Hole mobility

Besides the absorption and energy levels, the charge carrier transport abilities of polymers have also great an important effect on the resulting photovoltaic performance of PSCs, especially on FF.[34,40] We measured the hole-only mobilities (μ_h) of PBDTDT(Qx-3)-T blended with $PC_{71}BM$ at an optimized blend ratio ($w{:}w$, 1:4) under different conditions by the space charge limited current (SCLC) method with a device structure of ITO/PEDOT:PSS/polymer:$PC_{71}BM$/Au. The SCLC could be estimated using the Mott-Gurney equation: $J = (9/8)\varepsilon_0\varepsilon_r\mu_h(V/L^3)$,[41] where, J is current density, ε_r is dielectric constant of terpolymer, ε_0 is free-space permittivity (8.85 × 10^{-12} F/m), L is thickness of the blended film layer (105 nm), $V = V_{appl} - V_{bi}$, V is the effective voltage, V_{appl} is applied voltage, and V_{bi} is built-in voltage that results from

the work function difference between the anode and cathode. As shown in Fig. 4, the

hole-only mobilities of PBDTDT(Qx-3)-T are calculated to be 1.01×10^{-4}, 1.53×10^{-4}

and 2.19×10^{-4} cm^2 V^{-1} s^{-1} in the hole-only polymer/PC$_{71}$BM-based devices, under

without annealing, annealing temperature of 80 $^{\circ}$C, and annealing temperature of

80 $^{\circ}$C with 1% DIO additive conditions, respectively. Compared to the previous

BDT-T-*alt*-DTQx polymers,[32-34] PBDTDT(Qx-3)-T shows a best hole mobility under

annealing temperature of 80 $^{\circ}$C with 1% DIO additive condition, which implies that

the relatively a higher *FF* could be obtained in the PSCs.[13,42]

3.5. Photovoltaic properties

To investigate the photovoltaic properties of the polymer, the BHJ-PSCs were also

fabricated with a typical device structure of ITO/PEDOT:PSS/active layer/Ca/Al. The

active layer of PBDTDT(Qx-3)-T/PC$_{71}$BM with a thickness of 105 nm was obtained

from an ODCB solution at a concentration of 35 mg/mL. The photovoltaic

performances of PSCs are strongly affected by the processing parameters,[42] and these

processing parameters were investigated to optimize the photovoltaic performance of

PBDTDT(Qx-3)-T. To obtain the optimal D/A (PBDTDT(Qx-3)-T/PC$_{71}$BM, *w/w*)

ratios, annealing temperature, DIO additive concentration and spin-coating rates on

the photovoltaic properties, the current density-voltage *(J-V)* characteristics of

PBDTDT(Qx-3)-T/PC$_{71}$BM based devices at different ratios, annealing temperatures,

DIO additive and spin-coating rates are showed in Fig. S1, S2, S3, and S4,

respectively. The resulting photovoltaic data are summarized in Tables S1, S2, S3 and

S4, respectively. Successfully, an optimized PBDTDT-(Qx-3)-T/PC$_{71}$BM ratio of 1:4,

annealing temperature of 80 °C, DIO additive concentration of 1% and spin-coating rate of 2250 rpm were obtained in the BHJ-PSCs. As shown in Fig. 5, three typical devices exhibited the typical *J-V* characteristics under different conditions, and the device parameters, such as J_{sc}, V_{oc}, *FF* and PCE were summarized in Table 3. More encouragingly, all of the three typical devices exhibit excellent photovoltaic properties.

Without any post fabrication treatment, the device performances exhibited moderate PCE of 5.8%. When we used the annealed active layer, the device performances were moderate improved, which can be attributed to the increased J_{sc} value and well-controlled nanoscale morphology of the BHJ active layer films lead to an improved efficient photo-response (see Fig. 6 and Fig. 7). The corresponding PCE was increased to 6.2% with a comparable V_{oc} value of 0.96 V and a J_{sc} of 11.10 mA cm^{-2}. When further treated with 1% DIO additive, the device performances were greatly enhanced and exhibited a high PCE of 6.9%, which can be attributed to the increased *FF* value of 64.7% and same well-optimized nanoscale morphology of the BHJ active layer films lead to a enhancive hole mobility. As result, the maximum PCE of up to 6.9% with a V_{oc} of 0.94 V, a J_{sc} of 11.28 mA cm^{-2} and a *FF* of 64.7% was obtained in the PBDTDT(Qx-3)-T/PC$_{71}$BM-based device. To our knowledge, the recorded maximum PCE and *FF* values here are highest than those of the previous BDT-T-*alt*-DTQx based on copolymeric derivatives in BHJ-PSCs, due to the side chains modified engineering and the device optimization.[32-34]

To understand why the PBDTDT(Qx-3)-T/PC$_{71}$BM based devices displayed high

PCE values, external quantum efficiency (*EQE*) curves of devices under the different

conditions were also measured. As depicted in Fig. 6, the PBDTDT(Qx-3)-T/PC$_{71}$BM

based three devices show very efficient photo-response in a broad range from 310 to

730 nm, corresponding to high *EQE* over 40% in a broad range from 340 to 630 nm is

observed for all three devices. The maximum *EQE* of 73% at 420 nm for the device

without annealing, 76% at 422 nm for the device with annealing temperature of 80 $^{\circ}$C,

and 80% at 431 nm for the device with annealing temperature of 80 $^{\circ}$C and 1% DIO

additive, respectively. These differences can be attributed to changes of the surface

morphologies.[29] Obviously, high *EQE* value is responsible for high J_{sc} of

PBDTDT(Qx-3)-T based PSCs. According to the *EQE* curves and the solar irradiation

spectrum, the integral J_{sc} values of the PBDTDT(Qx-3)-T based PSCs are 10.45,

10.96 and 11.30 mA cm^{-2}, respectively, which are coincident with the measured J_{sc}

values within a 2% error.

3.6. Morphology

To better understand the photovoltaic performances of the resulting polymer,

tapping mode atomic force microscope (AFM) measurements are carried out to

demonstrate the surface morphologies of the blend films of PBDTDT(Qx-3)-T/

PC$_{71}$BM (1:4, *w/w*) processed in unannealed, annealed and annealed with DIO

additive, and the height images (5 × 5 μm^2) are showed in Fig. 6. The root mean

square (RMS) roughness is observed to be 1.45 nm in unannealed conditions, and the

other blend films after annealing and adding DIO additive exhibit smooth surface and

the RMS are 0.83 and 0.45 nm, respectively. In general, good surface morphology is

available to enhance photovoltaic performance. The results agreed well with the improvement of J_{sc} from 10.50 to 11.28 mA cm^{-2} for the PBDTDT(Qx-3)-T based PSCs. Thus, the well-ordered nanoscale morphology of PBDTDT(Qx-3)T/PC$_{71}$BM should also result in high charge carrier mobility, which gives rise to *FF* of 64.7%, better device performance with a PCE up to 6.9%. Therefore, the relatively excellent morphology together with the high hole mobility mentioned above, results in a high J_{sc} and *FF*.

4. Conclusions

A novel D-A-type polymer of PBDTDT(Qx-3)-T was obtained with BDT-T-*alt*-DTQx building block to investigate the influence of side chains at quinoxaline on the photovoltaic performances. The polymer exhibited a high decomposition temperature of 357 °C, broad absorption in the range of 300-696 nm, a low-lying HOMO energy level of -5.51 eV, and a high carrier mobility of 2.19×10^{-4} cm^2 V^{-1} s^{-1}. Based on the PBDTDT(Qx-3)-T/PC$_{71}$BM blend, the device exhibited an outstandingly increasing V_{oc} value of 0.96 V and a maximum PCE value of 6.9% with a V_{oc} of 0.94 V, a J_{sc} of 11.28 mA cm^{-2}, and a *FF* of 64.7%. The maximum PCE and *FF* values here are highest level in the reported the BDT-T-*alt*-DTQx copolymeric derivatives based PSCs. Our work demonstrates that photovoltaic properties of the BDT-T-*alt*-DTQx based polymers in PSCs can be remarkably increased by the side chains modified engineering, in which just appending two octyloxy side chains at 6,7-positions of quinoxaline.

Acknowledgements

Notes and references

1. L. Ye, S. Zhang, L. Huo, M. Zhang and J. Hou, *Acc. Chem. Res.*, 2014, **47**, 1595.

2. P. Bujak, I. K. Bajer, M. Zagorska, V. Maurel, I. Wielgus and A. Pron, *Chem. Soc. Rev.*, 2013, **42**, 8895.

3. Y. Li. *Acc. Chem. Res.*, 2012, **45**, 723.

4. M. Wang, H. Wang, T. Yokoyama, X. Liu, Y. Huang, Y. Zhang, T. Q. Nguyen, S. Aramaki and G. C. Bazan, *J. Am. Chem. Soc.*, 2014, **136**, 12576.

5. J. Yuan, L. Xiao, B. Liu, Y. Li, Y. He, C. Pan and Y. Zou, *J. Mater. Chem. A*, 2013, **1**, 10639.

6. Q. Fan, Y. Liu, M. Xiao, H. Tan, Y. Wang, W. Su, D. Yu, R. Yang and W. Zhu, *Org. Electron.*, 2014, **15**, 3375.

7. D. Ouyang, M. Xiao, D. Zhu, W. Zhu, Z. Du, N. Wang, Y. Zhou, X. Bao and R. Yang, *Polym. Chem.*, 2015, **6**, 55.

8. G. Li, C. Kang, X. Gong, J. Zhang, C. Li, Y. Chen, H. Dong, W. Hu, F. Li and Z.

Bo, *Macromolecules*, 2014, **47**, 4645.

9. S. Li, B. Zhao, Z. He, S. Chen, J. Yu, A. Zhong, R. Tang, H. Wu, Q. Li, J. Qin and Z. Li, *J. Mater. Chem. A*, 2013, **1**, 4508.

10. Y. Liu, J. Zhao, Z. Li, C. Mu, W. Ma, H. Hu, K. Jiang, H. Lin, H. Ade and H. Yan, *Nat. commun.*, 2014, **5**, 6293.

11. J. Warnan, C. Cabanetos, R. Bude, A. E. Labban, L. Li and P. M. Beaujuge, *Chem. Mater.*, 2014, **26**, 2829.

12. J. M. Jiang, H. C. Chen, H. K. Lin, C. M. Yu, S. C. Lan, C. M. Liu and K. H. Wei, *Polym. Chem.*, 2013, **4**, 5321.

13. W. Li, S. Albrecht, L. Yang, S. Roland, J. R. Tumbleston, T. McAfee, L. Yan, M. A. Kelly, H. Ade, D. Neher and W. You, *J. Am. Chem. Soc.*, 2014, **136**, 15566.

14. A. Najari, P. Berrouard, C. Ottone, M. Boivin, Y. Zou, D. Gendron, W. O. Caron, P. Legros, C. N. Allen, S. Sadkin and M. Leclerc, *Macromolecules*, 2012, **45**, 1833.

15. N. I. Abdo, J. Ku, A. A. E. Shehawy, H. S. Shim, J. K. Min, A. A. E. Barbary, Y. H. Jang and J. S. Lee, *J. Mater. Chem. A*, 2013, **1**, 10306.

16. E. T. Hoke, K. Vandewal, J. A. Bartelt, W. R. Mateker, J. D. Douglas, R. Noriega, K. R. Graham, J. M. J. Fréchet, A. Salleo and M. D. McGehee, *Adv. Energy Mater.*, 2013, **3**, 220.

17. H. Li, S. Sun, S. Mhaisalkar, M. T. Zin, Y. M. Lam and A. C. Grimsdale, *J. Mater. Chem. A*, 2014, **2**, 17925.

18. Q. Liu, Z. Du, W. Chen, L. Sun, Y. Chen, M. Sun and R. Yang, *Synthetic Met.*, 2013, **178**, 38.

19. S. Q. Zhang, L. Ye, W. C. Zhao, B. Yang, Q. Wang and J. H. Hou, *Sci. China Chem.*, 2015, **58**, 248.

20. L. Dou, J. Gao, E. Richard, J. You, C. C. Chen, K. C. Cha, Y. He, G. Li and Y. Yang, *J. Am. Chem. Soc.*, 2012, **134**, 10071.

21. L. Ye, S. Zhang, W. Zhao, H. Yao and J. Hou, *Chem. Mater.*, 2014, **26**, 3603.

22. T. Qin, W. Zajaczkowski, W. Pisula, M. Baumgarten, M. Chen, M. Gao, G. Wilson, C. D. Easton, K. Müllen and S. E. Watkins, *J. Am. Chem. Soc.*, 2014, **136**, 6049.

23. S. H. Liao, H. J. Jhuo, Y. S. Cheng and S. A. Chen, *Adv. Mater.*, 2013, **25**, 4766.

24. Y. Wang, Y. Liu, S. Chen, R. Peng and Z. Ge, *Chem. Mater.*, 2013, **25**, 3196.

25. J. M. Jiang, H. K. Lin, Y. C. Lin, H. C. Chen, S. C. Lan, C. K. Chang and K. H. Wei, *Macromolecules*, 2014, **47**, 70.

26. H. J. Song, D. H. Kim, E. J. Lee and D. K. Moon, *J. Mater. Chem. A*, 2013, **1**, 6010.

27. J. H. Kim, C. E. Song, H. U. Kim, A. C. Grimsdale, S. J. Moon, W. S. Shin, S. K. Choi and D. H. Hwang, *Chem. Mater.*, 2013, **25**, 2722.

28. D. Dang, W. Chen, S. Himmelberger, Q. Tao, A. Lundin, R. Yang, W. Zhu, A. Salleo, C. Müller and E. Wang, *Adv. Energy Mater.*, 2014, **4**, 00680.

29. H. C. Chen, Y. H. Chen, C. C. Liu, Y. C. Chien, S. W. Chou and P. T. Chou, *Chem. Mater.*, 2012, **24**, 4766.

30. H. C. Chen, Y. Chen, C. Liu, Y. H. Hsu, Y. C. Chien, W. T. Chuang, C. Y. Cheng, C. L. Liu, S. W. Chou, S. H. Tung and P. T. Chou, *Polym. Chem.*, 2013, **4**, 3411.

31. M. Tessarolo, D. Gedefaw, M. Bolognesi, F. Liscio, P. Henriksson, W. Zhuang, S.

Milita, M. Muccini, E. Wang, M. Seri and M. R. Andersson, *J. Mater. Chem. A*, 2014, **2**, 11162.

32. R. Duan, L. Ye, X. Guo, Y. Huang, P. Wang, S. Zhang, J. Zhang, L. Huo and J. Hou, *Macromolecules*, 2012, **45**, 3032.

33. D. Dang, M. Xiao, P. Zhou, J. Shi, Q. Tao, H. Tan, Y. Wang, X. Bao, Y. Liu, E. Wang, R. Yang and W. Zhu, *Org. Electron.*, 2014, **15**, 2876.

34. W. Su , M. Xiao, Q. Fan, J. Zhong, J. Chen, D. Dang, J. Shi, W. Xiong, X. Duan, H. Tan, Y. Liu and W. Zhu, *Org. Electron.*, 2015, **17**, 129.

35. S. Li, Z. He, J. Yu, S. Chen, A. Zhong, R. Tang, H. Wu, J. Qin and Z. Li, *J. Mater. Chem.*, 2012, **22**, 12523.

36. H. J. Song, D. H. Kim, E. J. Lee, J. R. Haw and D. K. Moon, *Sol. Energy Mater. Sol. Cells*, 2014, **123**, 112.

37. L. J. Lindgren, F. Zhang, M. Andersson, S. Barrau, S. Hellstrom, W. Mammo, E. Perzon, O. Inganas and M. R. Andersson, *Chem. Mater.*, 2009, **21**, 3491.

38. E. Wang, L. Hou, Z. Wang, Z. Ma, S. Hellstr€om, W. Zhuang, F. Zhang, O. Ingan€as and M. R. Andersson, *Macromolecules*, 2011, **44**, 2067.

39. Y. Li, Y. Cao, J. Gao, D. Wang, G. Yu and A. J. Heeger, *Synthetic Met.*, 1999, **99**, 243.

40. Z. G. Zhang and Y. F. Li, *Sci. China Chem.*, 2015, **58**, 192.

41. P. W. M. Blom, V. D. Mihailetchi, L. J. A. Koster and D. E. Markov, *Adv. Mater.*, 2007, **19**, 1551.

42. K. Li, Z. Li, X. Xu, L. Wang and Q. Peng, *J. Am. Chem. Soc.*, 2013, **135**, 13549.

Figures and Tables

Chart 1. Chemical structures of the BDT-T-*alt*-DTQx based polymers.

Scheme 1. Synthetic routes for the monomers and PBDTDT(Qx-3)-T.

Fig. 1. TGA curve of PBDTDT(Qx-3)-T at a scan rate of 20 $^{\circ}$C/min under nitrogen atmosphere.

Fig. 2. Normalized UV-Vis absorption spectra of PBDTDT(Qx-3)-T in dilute CHCl$_3$ and its neat film at RT.

Fig. 3. Cyclic voltammetry curve of PBDTDT(Qx-3)-T.

Fig. 4. *J-V* curves of the hole PBDTDT(Qx-3)-T/PC$_{71}$BM devices under different conditions.

Fig. 5. *J-V* curves of the PBDTDT(Qx-3)-T/PC$_{71}$BM-based PSCs at different conditions under illumination of AM1.5G, 100 mW cm^{-2}.

Fig. 6. *EQE* curves of the PBDTDT(Qx-3)-T/PC$_{71}$BM-based devices under the different conditions.

Fig. 7. AFM height images of the PBDTDT(Qx-3)-T/PC$_{71}$BM blend films in unannealed (a), annealed of 80 $^{\circ}$C (b), and annealed of 80 $^{\circ}$C with % DIO additive (c), respectively.

Table 1. Molecular weight and thermal properties of PBDTDT(Qx-3)-T.

Table 2. Optical and electrochemical properties of PBDTDT(Qx-3)-T.

Table 3. Photovoltaic properties of the polymers/PC$_{71}$BM-based PSCs at different conditions, under illumination of AM 1.5G, 100 mW cm^{-2}.
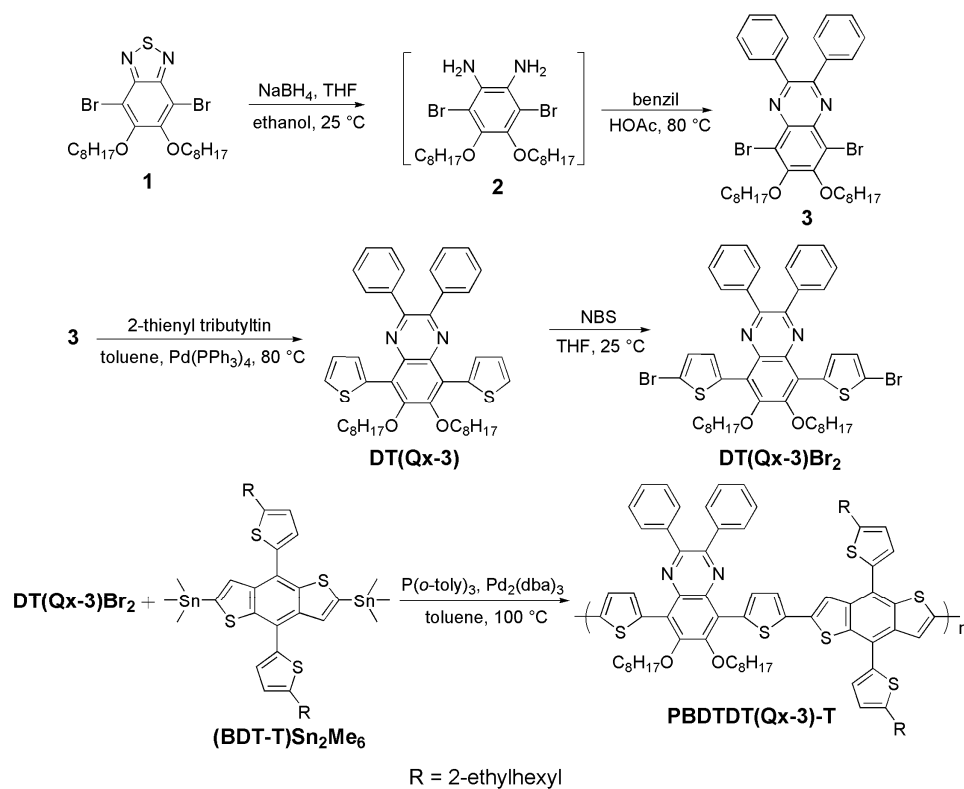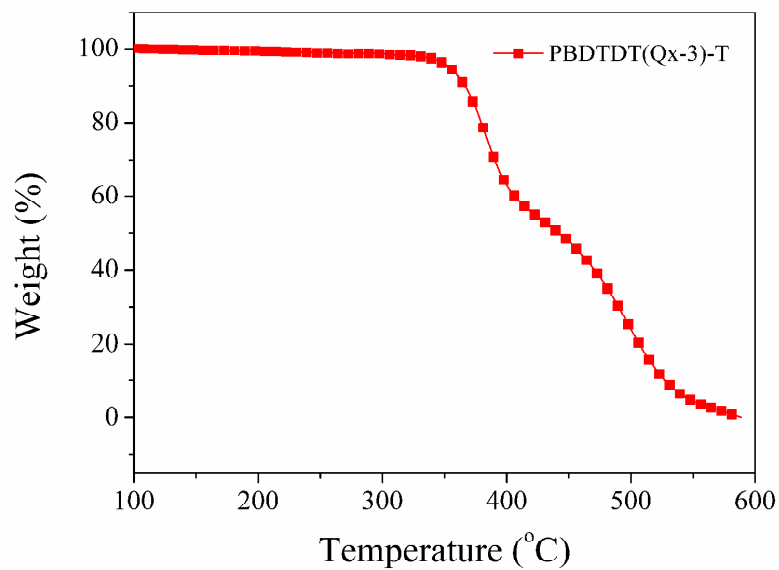
Chart 1

PBDTDTQx-T

PBDTDT(Qx-2)-T

PBDTT-TQ

PBDTDT(Qx-3)-T

R = 2-ethylhexyl

Scheme 1

R = 2-ethylhexyl
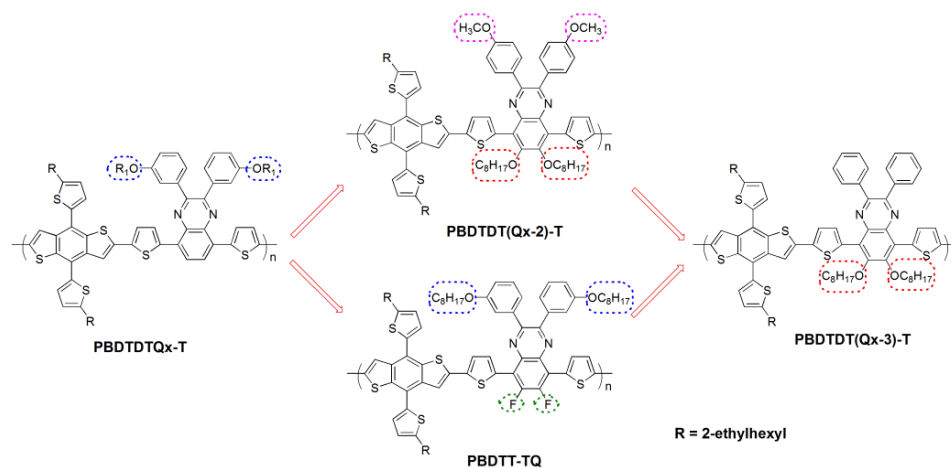
Fig. 1

Fig. 2
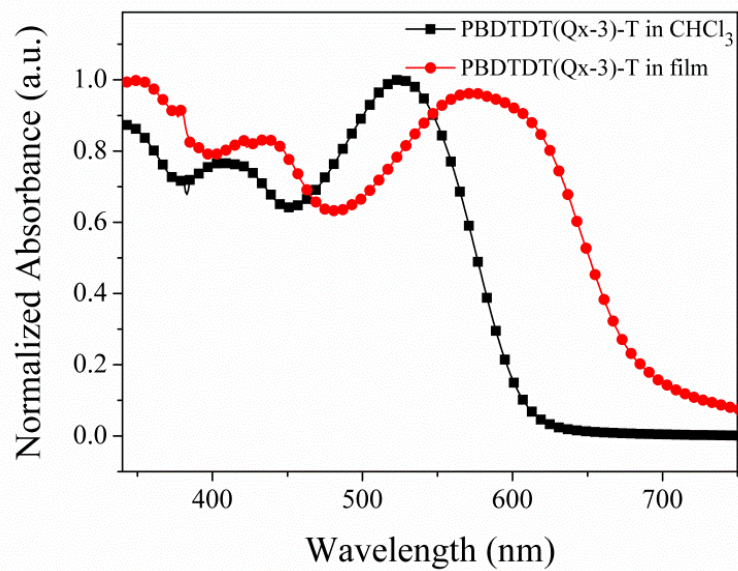
Fig. 3
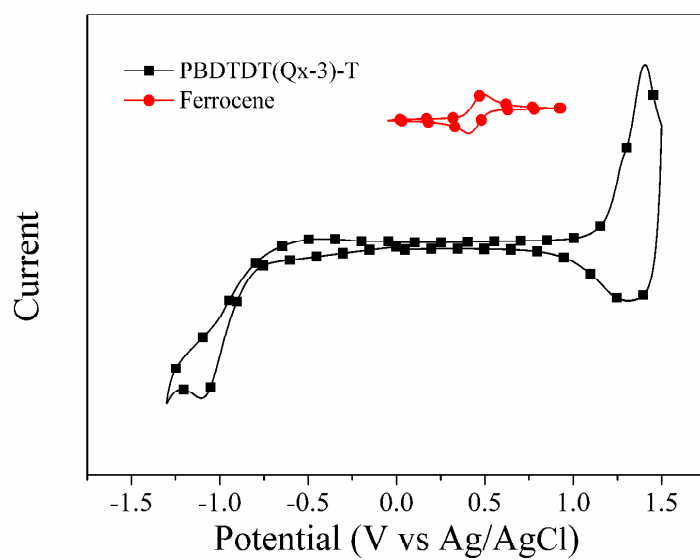
Fig. 4
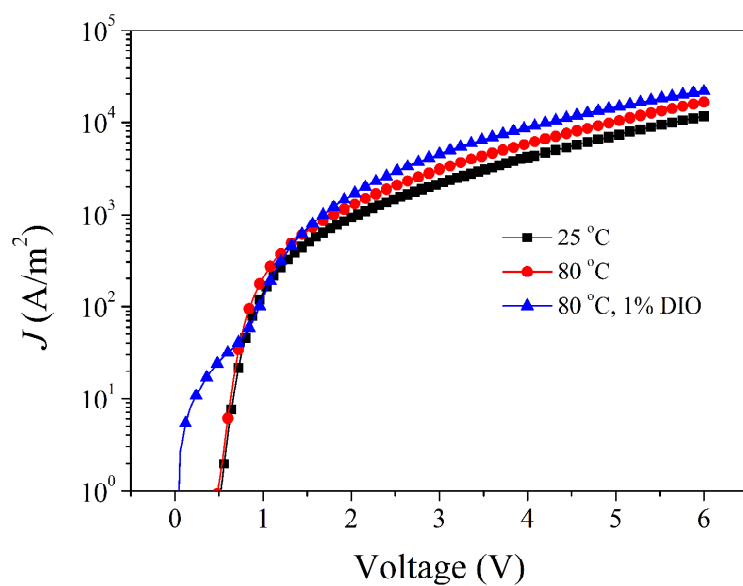
Fig. 5
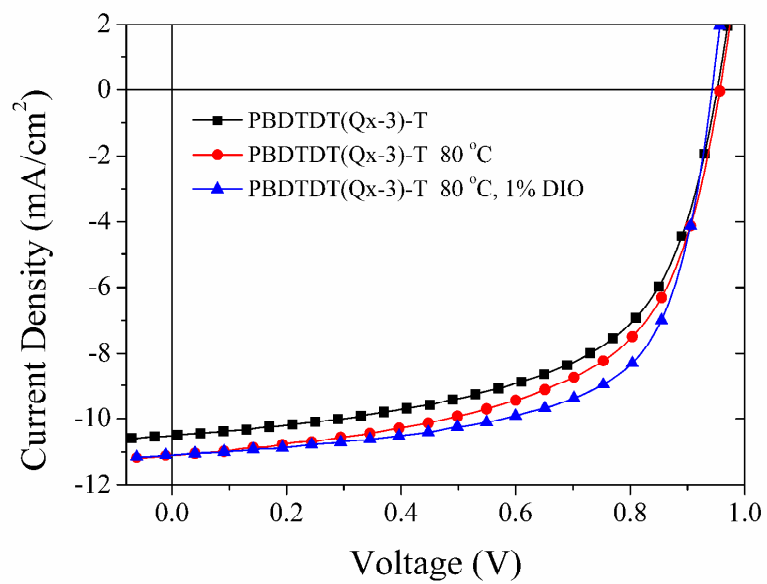
Fig. 6
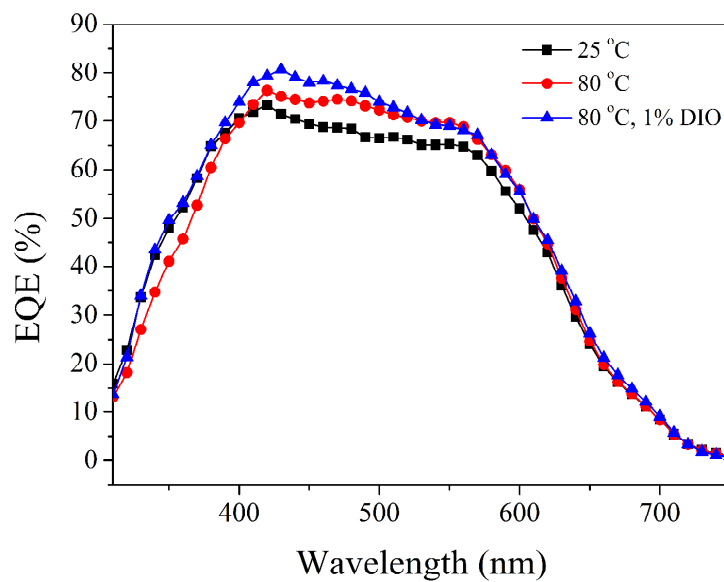
Fig. 7
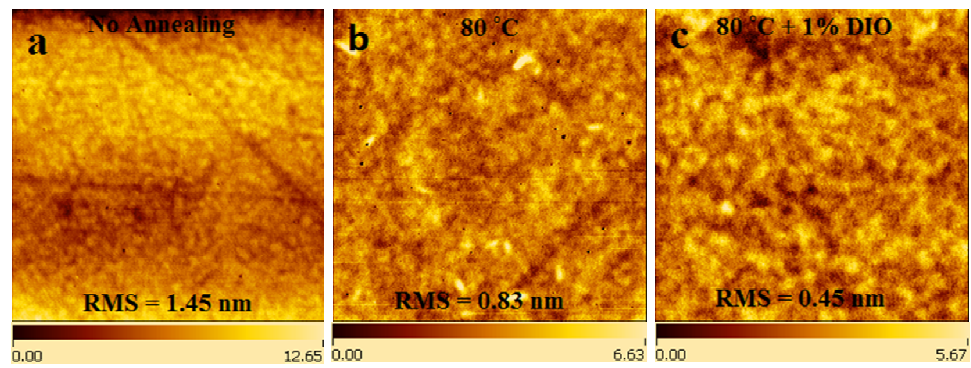
Table 1

Polymers	M_n (kDa)	M_w (kDa)	PDI	Yield (%)	T_d ($^\circ$C)
PBDTDT(Qx-3)-T	59	97	1.64	81.3	357

Table 2

Polymers	λ_{abs} [a] /nm	λ_{abs} [b] /nm	λ_{onset} [b] /nm	E_g^{opt} /eV	E_{HOMO} /eV	E_{LUMO} /eV	E_g^{ec} /eV	Ref.
PBDTDT(Qx-3)-T	408, 526	438, 577	696	1.78	-5.51	-3.57	1.94	This work
PBDTDT(Qx-2)-T	410, 521	420, 564	681	1.82	-5.41	-2.92	2.49	34
PBDTT-TQ	444, 630	447, 601	701	1.77	-5.45	-3.56	1.89	33
PBDTDTQx-T	443, 605	448, 605	740	1.67	-5.12	-3.45	1.67	32

[a] Measured in CHCl$_3$ solution. [b] Measured in the neat film.

Table 3

Polymers	J_{sc} /mA cm^{-2}	V_{oc} /V	FF /%	PCE$_{max}$ /%	μ_h /cm^2 V^{-1} s^{-1}	Ref.
PBDTDT(Qx-3)-T	10.50	0.95	58.5	5.8	1.01×10^{-4}	This work
PBDTDT(Qx-3)-T [a]	11.10	0.96	58.6	6.2	1.53×10^{-4}	This work
PBDTDT(Qx-3)-T [a,b]	11.28	0.94	64.7	6.9	2.19×10^{-4}	This work
PBDTDT(Qx-2)-T [a]	10.82	0.95	61.4	6.3	1.41×10^{-4}	34
PBDTT-TQ [c]	13.70	0.77	56.0	5.9	1.00×10^{-4}	33
PBDTDTQx-T [d]	10.13	0.76	64.3	5.0	1.04×10^{-4}	32

[a] Annealing at 80 $^\circ$C; [b] 1% DIO additive; [c] Annealing at 90 $^\circ$C; [d] Annealing at 120 $^\circ$C.